INTERNATIONAL ATOMIC ENERGY AGENCY
UNITED NATIONS EDUCATIONAL, SCIENTIFIC AND CULTURAL ORGANIZATION
INTERNATIONAL CENTRE FOR THEORETICAL PHYSICS
I.C.T.P., P.O. BOX 586, 34100 TRIESTE, ITALY. CABLE CENTRATOM TRIESTE

UNITED NATIONS INDUSTRIAL DEVELOPMENT ORGANIZATION

INTERNATIONAL CENTRE FOR SCIENCE AND HIGH TECHNOLOGY

SMR/548-16

Course on Oceanography of Semi-Enclosed Seas
15 April - 3 May 1991

"Shallow Sea Modelling"

J. WOLF
Proudman Oceanographic Laboratory
Bidston Observatory
Merseyside, U.K.

Please note: These notes are intended for internal distribution only

ICTP COURSE ON OCEANOGRAPHY OF SEMI-ENCLOSED SEAS

SHALLOW SEA MODELLING

J. WOLF
Proudman Oceanographic Laboratory
Bidston Observatory
Birkenhead
Merseyside
U.K. L43 7RA

1. Shallow sea oceanography

1.1 Introduction
1.2 Derivation of equations
1.3 The hydrostatic approximation
1.4 Time-averaging and the Reynolds' stresses
1.5 The Boussinesq approximation
1.6 Density equations
1.7 Advective terms
1.8 Depth-averaged equations

2. Models

2.1 Types of model
2.2 Analytic models
2.3 Physical models
2.4 Numerical models
2.5 Partial differential equations
2.6 Finite elements
2.7 Finite differences
2.8 Consistency, convergence and stability
2.9 Explicit vs. implicit methods

3. Finite difference modelling

3.1 An explicit 2D tide/surge model
3.2 Coordinate system
3.3 Nonlinear effects
3.4 Initial and boundary conditions
3.5 Grid selection
3.6 Tides and surges
3.7 Wind forcing and atmospheric pressure effects
3.8 Friction
3.9 Finite difference solution

4. Shallow sea models

4.1 2D tide/surge/wave model
4.2 3D tidal models
4.3 A density-evolving frontal model
4.4 Turbulence energy modelling
4.5 An idealised shelf edge model
4.6 Water quality modelling: the North Sea
4.7 Lagrangian particle-tracking models
4.8 Summary

1. Shallow sea oceanography

1.1 Introduction

These lectures aim to highlight those processes in physical oceanography which are specific to shallow seas. By shallow seas are meant water bodies of less than 200m depth and usually much less than 100m deep. They include continental shelves whether wide (as in Northern Europe) or narrow (as in the Pacific coast of U.S.A.) and partially or fully enclosed seas like the North Sea and the North American Great Lakes. Changes in sea level relative to water depth are not negligible and the wavelengths of the dominant motions are much larger than the water depth. Vertical velocities are relatively small and usually negligible. This topic is well described by Csanady (1982).

It is intended to put forward specific examples placed in their general context. The equations of motion are derived with suitable approximations for shallow seas. Various types of model are discussed before concentrating on numerical models, and in particular finite difference models. Some details of finite difference methods are discussed, followed by detailed application to storm surge modelling on the UK continental shelf. Finally, a range of examples of numerical models is given, modelling different processes and using different techniques, each of which is described briefly.

1.2 Derivation of equations

The fundamental equations may be expressed in either an Eulerian or a Lagrangian frame of reference. The former describes motion relative to a fixed point in space while the latter describes the movement of individual particles. We will use the Eulerian frame of reference exclusively for the following derivations although the Lagrangian frame is particularly useful in particle-tracking dispersion models, as discussed in §4. The Cartesian coordinate system used generally is shown in Fig. 1.1.

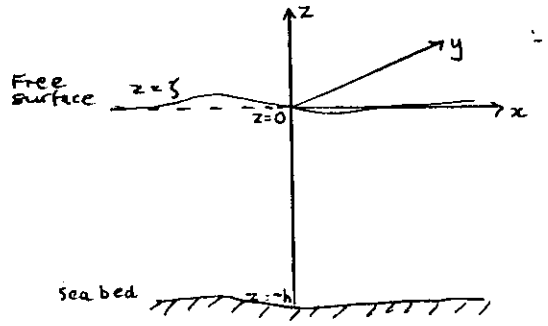

Fig. 1.1

Here, x and y are orthogonal axes in the plane of the undisturbed water surface, z is positive upwards and t is time.

The Cartesian coordinate system will be used for simplicity, however it is only a special case of an orthogonal curvilinear coordinate system. The derivations will be given first in vector notation, which is independent of the coordinate system used, before being recast in the Cartesian system for clarity. Other coordinate systems may be used (see §3).

The law of conservation of mass, stating that a local change in mass is due only to a divergence of the mass flux may be stated

$$\frac{\partial \rho}{\partial t} + \nabla \cdot (\rho \underset{\sim}{q}) = 0 \qquad (1.1)$$

where ρ is the density and $\underset{\sim}{q}$ the velocity vector. If the fluid is incompressible density differences are much less than the effects of velocity gradients in shallow seas then this reduces to

$$\nabla \cdot \underset{\sim}{q} = 0 \qquad (1.2)$$

which is often called the continuity equation.

Newton's law of motion states that acceleration is equal to the force per unit mass, i.e. in a fixed frame of reference

$$\rho \frac{d\underset{\sim}{q}}{dt} = \rho \nabla \Phi - \nabla p + \underset{\sim}{F} \qquad (1.3)$$

where d/dt is the total acceleration $= \partial/\partial t + \underset{\sim}{q} \cdot \nabla$. The right hand side is the sum of the various forces acting on the sea, including the body force (or long-range force), $\rho \nabla \Phi$, and the surface (short-range) forces due to the pressure gradient, ∇p, and the shear stresses, $\underset{\sim}{F}$. In a Newtonian fluid the shear stress is linearly related to the velocity gradient by the molecular viscosity, μ. Equation (1.3) becomes (see Batchelor, 1967)

$$\rho \frac{d\underset{\sim}{q}}{dt} = \rho \nabla \Phi - \nabla p + 2(\nabla \cdot \mu \nabla)\underset{\sim}{q} - \frac{2}{3}\nabla(\mu \nabla \cdot \underset{\sim}{q}) + \nabla \times (\mu \nabla \times \underset{\sim}{q}) \qquad (1.4)$$

Introducing the continuity equation (1.2) and assuming the molecular viscosity to be a constant (which is the case if the temperature differences are small as they are in the sea) we get

$$\frac{d\underset{\sim}{q}}{dt} = \nabla \Phi - \frac{\nabla p}{\rho} + \nu \nabla^2 \underset{\sim}{q} \qquad (1.5)$$

using $\nabla^2 \underset{\sim}{q} = \nabla(\nabla \cdot \underset{\sim}{q}) - \nabla \times (\nabla \times \underset{\sim}{q})$

and defining $\nu = \mu/\rho$, the kinematic viscosity.

In a frame of reference rotating with angular velocity $\underset{\sim}{\Omega}$ equation (1.5) becomes

$$\frac{d\underset{\sim}{q}}{dt} + 2\underset{\sim}{\Omega} \times \underset{\sim}{q} = \nabla \Phi' - \frac{\nabla p}{\rho} + \nu \nabla^2 \underset{\sim}{q} \qquad (1.6)$$

where $\Phi' = \Phi + |\underset{\sim}{\Omega} \times \underset{\sim}{x}|/2$, with $\underset{\sim}{x}$ the position vector. The second part of this term comes from the centripetal acceleration $\underset{\sim}{\Omega} \times (\underset{\sim}{\Omega} \times \underset{\sim}{x})$ (Pedlosky, 1979, p.19). The surface of the Earth is an equipotential surface, i.e. Φ' is a constant, and the body force is usually due to gravity alone. $\nabla \Phi'$ is then the effective gravitational acceleration, $\underset{\sim}{g}$, which includes the centripetal

acceleration due to the Earth's rotation, hence the equation is usually written

$$\frac{d\underset{\sim}{q}}{dt} + 2\underset{\sim}{\Omega} \times \underset{\sim}{q} = \underset{\sim}{g} - \frac{\nabla p}{\rho} + \nu \nabla^2 \underset{\sim}{q} . \qquad (1.7)$$

The 'apparent' acceleration in the second term on the left hand side, due to the rotating frame of reference, is called the Coriolis acceleration. The equation (1.7) may be written in Cartesian coordinates

$$\frac{du}{dt} - 2(\Omega_z v - \Omega_y w) = -\frac{1}{\rho}\frac{\partial p}{\partial x} + \nu \nabla^2 u \qquad (1.8a)$$

$$\frac{dv}{dt} - 2(\Omega_x w - \Omega_z u) = -\frac{1}{\rho}\frac{\partial p}{\partial y} + \nu \nabla^2 v \qquad (1.8b)$$

$$\frac{dw}{dt} - 2(\Omega_y u - \Omega_x v) = -g - \frac{1}{\rho}\frac{\partial p}{\partial z} + \nu \nabla^2 w \qquad (1.8c)$$

where Ω_x, Ω_y and Ω_z are the components of the Earth's angular velocity in the x, y and z directions respectively.

1.3 The hydrostatic approximation

In shallow water in particular, the vertical velocity components and accelerations are much smaller than gravity, for example, and the Coriolis acceleration is also small. The vertical equation of motion (1.8c) reduces to

$$\frac{1}{\rho}\frac{\partial p}{\partial z} = -g \qquad (1.9)$$

which is equivalent to the balance of forces in a stationary fluid (hence 'hydrostatic').

Similarly the vertical velocity in the Coriolis terms can be neglected so that we have, from (1.8a) and (1.8b)

$$\frac{du}{dt} - fv = -\frac{1}{\rho}\frac{\partial p}{\partial x} + \nu \nabla^2 u \qquad (1.10a)$$

$$\frac{dv}{dt} + fu = -\frac{1}{\rho}\frac{\partial p}{\partial y} + \nu \nabla^2 v \qquad (1.10b)$$

writing $f = 2\omega \sin\phi$, the Coriolis parameter; $\omega = |\underset{\sim}{\Omega}|$, ϕ is latitude.

1.4 Time-averaging and the Reynolds' stresses

The scales of motion which we want to examine are much larger than the molecular scale and it is usual to separate the dependent variables into mean and fluctuating components and average the equations over a suitable time interval. The following derivation is given without consideration of the complexities of the averaging procedure, assuming the mean flow and turbulent flow time scales are well separated.

Let $u = [u] + u'$, $v = [v] + v'$, $w = [w] + w'$ and $p = [p] + p'$

where [] denotes the time average, $[u'] = 0$ etc.
The equations of motion and continuity become

$$\frac{\partial [u]}{\partial x} + \frac{\partial [v]}{\partial y} + \frac{\partial [w]}{\partial z} = 0 , \qquad (1.11a)$$

$$\frac{d[u]}{dt} - f[v] = -\frac{1}{\rho}\frac{\partial [p]}{\partial x} + \frac{1}{\rho}\left\{\frac{\partial}{\partial x}\tau_{xx} + \frac{\partial}{\partial y}\tau_{yx} + \frac{\partial}{\partial y}\tau_{zx}\right\} , \qquad (1.11b)$$

$$\frac{d[v]}{dt} + f[u] = -\frac{1}{\rho}\frac{\partial [p]}{\partial y} + \frac{1}{\rho}\left\{\frac{\partial}{\partial x}\tau_{xy} + \frac{\partial}{\partial y}\tau_{yy} + \frac{\partial}{\partial z}\tau_{zy}\right\} , \qquad (1.11c)$$

$$g = -\frac{1}{\rho}\frac{\partial [p]}{\partial z} , \qquad (1.11d)$$

where $\tau_{xx} = -\rho[u'^2] + 2\mu\frac{\partial [u]}{\partial x}$, $\tau_{xy} = \tau_{yx} = -\rho[u'v'] + \mu\left(\frac{\partial [v]}{\partial x} + \frac{\partial [u]}{\partial y}\right)$,

$\tau_{yy} = -\rho[v'^2] + 2\mu\frac{\partial [v]}{\partial y}$, $\tau_{zy} = -\rho[v'w'] + \mu\left(\frac{\partial [w]}{\partial y} + \frac{\partial [v]}{\partial z}\right)$,

$\tau_{zx} = -\rho[u'w'] + \mu\left(\frac{\partial [w]}{\partial x} + \frac{\partial [u]}{\partial z}\right)$;

$\rho[u'^2]$, $\rho[u'v']$ etc. are called the Reynolds' stresses or turbulent stresses. In shallow seas the flow is usually turbulent at least in the surface and bottom boundary layers, which form a significant fraction of the water column. Whether or not the flow is turbulent may be determined from the Reynolds number for a given flow, $R_e = UD/\nu$, where U and D are characteristic velocity and length scales. This describes the ratio between the turbulent and molecular stresses.

In order to solve the equations for the mean flow the shear stresses must be related to some properties of the mean flow, either directly or by including further conservation equations in the turbulent quantities. This is a difficult problem with no exact solution. The simplest approach is given here, other treatments are mentioned in §4.

The most common treatment is to relate the turbulent stresses to gradients of the mean flow, introducing a quantity called eddy viscosity, analogous to molecular viscosity. This gives

$$\frac{du}{dt} - fv = -\frac{1}{\rho}\frac{\partial p}{\partial x} + \frac{\partial}{\partial x}\left(N_x\frac{\partial u}{\partial x}\right) + \frac{\partial}{\partial y}\left(N_y\frac{\partial u}{\partial y}\right) + \frac{\partial}{\partial z}\left(N_z\frac{\partial u}{\partial z}\right) \qquad (1.12a)$$

$$\frac{dv}{dt} + fu = -\frac{1}{\rho}\frac{\partial p}{\partial y} + \frac{\partial}{\partial x}\left(N_x\frac{\partial v}{\partial x}\right) + \frac{\partial}{\partial y}\left(N_y\frac{\partial v}{\partial y}\right) + \frac{\partial}{\partial z}\left(N_z\frac{\partial v}{\partial z}\right) \qquad (1.12b)$$

having dropped [] for clarity.

These equations are commonly described as the 'shallow water equations'.

Here N_x and N_y are components of the horizontal eddy viscosity and N_z is the vertical eddy viscosity. These are not constants but also vary with the mean velocity gradients so N_z is the larger, since the vertical scale is much shorter than the horizontal. Eddy viscosity is sometimes set to a constant value to obtain a simple solution, but this is not very realistic.

1.5 The Boussinesq approximation

Density variations in a shallow sea may be regarded as perturbations about a mean level $\rho = \rho_0(1+\epsilon)$. Density variations are typically of the order of one part per thousand.

Integrating the hydrostatic pressure formula with respect to z

$$p = p_a + \int_z^\zeta \rho g \, dz \qquad (1.13)$$

$$\frac{\partial p}{\partial x} = \frac{\partial p_a}{\partial x} + \rho_s g \frac{\partial \zeta}{\partial x} + \int_z^\zeta g \frac{\partial \rho}{\partial x} dz \qquad (1.14)$$

where p_a = atmospheric pressure, $z = \zeta$ is the free surface elevation, ρ_s the surface density $\approx \rho_0$ so

$$\frac{1}{\rho_0}\frac{\partial p}{\partial x} = \frac{1}{\rho_0}\frac{\partial p_a}{\partial x} + g\frac{\partial \zeta}{\partial x} + \frac{1}{\rho_0}\int_z^\zeta g \frac{\partial \rho}{\partial x} dz \qquad (1.15)$$

ignoring ϵ except in the density gradient term. This is called the Boussinesq approximation.

1.6 Density equations

Conservation laws for temperature and salinity may be set up from which the density is calculated in an equation of state. Thus

$$\frac{dT}{dt} = -\nabla\cdot\left(\frac{\underset{\sim}{Q}}{\rho c_p}\right) \qquad (1.16)$$

T is temperature, $\underset{\sim}{Q}$ is the heat flux including Reynolds' fluxes [u'T'] etc., c_p is specific heat.

$$\frac{dS}{dt} = -\nabla\cdot\left(\frac{\underset{\sim}{s}}{\rho}\right) \qquad (1.17)$$

where S is salinity, $\underset{\sim}{s}$ is salt flux including Reynolds' fluxes [u'S'] etc.
Eddy diffusivities may be introduced analogous to molecular diffusivity as for eddy viscosity.

The equation of state specifies density as a function of S and T. Pressure effects on density can be ignored in shallow water.

$$\rho = \rho(T, S) \qquad (1.18)$$

1.7 Advective terms

The total time derivative is

$$\frac{du}{dt} \equiv \frac{\partial u}{\partial t} + u\frac{\partial u}{\partial x} + v\frac{\partial u}{\partial y} + w\frac{\partial u}{\partial z}$$
$$\equiv \frac{\partial u}{\partial t} + \frac{\partial(u^2)}{\partial x} + \frac{\partial(uv)}{\partial y} + \frac{\partial(uw)}{\partial z}$$

where the nonlinear terms containing the flow components are called advective terms, transporting momentum with the flow. They are generally small and in some instances can be neglected. In particular this may be true when the Rossby number (the ratio of nonlinear to Coriolis terms) is small. $R_o = U/fL$ where U and L are appropriate velocity and horizontal length scales. In near-coastal high-resolution models the Rossby number is typically of O(1) and the advection terms cannot strictly be neglected, but useful solutions can be obtained by linearising the equations, so they are often omitted.

1.8 Depth-averaged equations

In particular in shallow seas the vertical length scale is much smaller than the horizontal scale and for some wavelengths of interest e.g. tides and surges, is much smaller than the wavelength. Large tidal currents cause mixing which reduces stratification, leading to little vertical structure and in many applications the vertical structure is not required. It is then useful to integrate the equations through depth, simplifying the problem. The overbar has been used in the following derivation to denote depth-averaged quantities
e.g.

$$\bar{u} = \frac{1}{D}\int_{-h}^{\zeta} u \, dz, \quad \text{where } D = h+\zeta.$$

Integrating equations (1.11a), (1.12a) and (1.12b) over depth and ignoring density gradients we obtain

$$\frac{\partial}{\partial x}(D\bar{u}) + \frac{\partial}{\partial y}(D\bar{v}) + \frac{\partial \zeta}{\partial t} = 0 \qquad (1.19a)$$

$$\frac{\partial \bar{u}}{\partial t} + \frac{\partial(\bar{u}^2)}{\partial x} + \frac{\partial(\bar{u}\bar{v})}{\partial y} - f\bar{v} = -g\frac{\partial \zeta}{\partial x} - \frac{1}{\rho}\frac{\partial p_a}{\partial x} + \frac{F_s - F_B}{\rho D} \qquad (1.19b)$$

$$\frac{\partial \bar{v}}{\partial t} + \frac{\partial(\bar{u}\bar{v})}{\partial x} + \frac{\partial(\bar{v}^2)}{\partial y} + f\bar{u} = -g\frac{\partial \zeta}{\partial y} - \frac{1}{\rho}\frac{\partial p_a}{\partial y} + \frac{G_s - G_B}{\rho D} \qquad (1.19c)$$

$D = (h + \zeta)$ is the total water depth. We have used the kinematic boundary conditions

$$\frac{d}{dt}(z-\zeta) = 0 \quad \text{i.e.} \quad w(\zeta) - u(\zeta)\frac{\partial \zeta}{\partial x} - v(\zeta)\frac{\partial \zeta}{\partial y} - \frac{\partial \zeta}{\partial t} = 0 \quad \text{at } z = \zeta$$

$$\frac{d}{dt}(z+h) = 0 \quad \text{i.e.} \quad w(-h) + u(-h)\frac{\partial h}{\partial x} + v(-h)\frac{\partial h}{\partial y} = 0 \quad \text{at } z = -h$$

and Leibniz' rule for integration with variable limits, so that, for example, $\int_{-h}^{\zeta}\frac{\partial u}{\partial x}dz = \frac{\partial}{\partial x}\int_{-h}^{\zeta} u\,dz - u(\zeta)\frac{\partial \zeta}{\partial x} - u(-h)\frac{\partial h}{\partial x}$.

The horizontal shear stress terms have been omitted for now.

$$F_s = \tau_{zx}(\zeta) - \tau_{xx}(\zeta)\frac{\partial \zeta}{\partial x} - \tau_{xy}(\zeta)\frac{\partial \zeta}{\partial y}$$

and $$G_s = \tau_{zy}(\zeta) - \tau_{xy}(\zeta)\frac{\partial \zeta}{\partial x} - \tau_{yy}(\zeta)\frac{\partial \zeta}{\partial y}$$

are components of surface stress (wind-stress) at the sea surface, $z = \zeta$.

$$F_B = \tau_{zx}(-h) + \tau_{xx}(-h)\frac{\partial h}{\partial x} + \tau_{xy}(-h)\frac{\partial h}{\partial y}$$

And $$G_B = \tau_{zy}(-h) + \tau_{xy}(-h)\frac{\partial h}{\partial x} + \tau_{yy}(-h)\frac{\partial h}{\partial y}$$

are the components of stress at the sea-bed $z = -h$.

The advective terms may be re-written so that

e.g. $$\frac{\partial(\bar{u}^2)}{\partial x} = \frac{\partial}{\partial x}\left\{\bar{u}^2 + \overline{(u-\bar{u})^2}\right\}$$

We can then write, in full,

$$\frac{\partial \bar{u}}{\partial t} + \bar{u}\frac{\partial \bar{u}}{\partial x} + \bar{v}\frac{\partial \bar{u}}{\partial y} - f\bar{v} = -g\frac{\partial \zeta}{\partial x} - \frac{1}{\rho}\frac{\partial p_a}{\partial x} + \frac{F_S - F_B}{\rho D} + \frac{1}{\rho D}\frac{\partial}{\partial x}(DM_{xx}) + \frac{1}{\rho D}\frac{\partial}{\partial y}(DM_{yx}) \quad (1.20)$$

and $$\frac{\partial \bar{v}}{\partial t} + \bar{u}\frac{\partial \bar{v}}{\partial x} + \bar{v}\frac{\partial \bar{v}}{\partial y} + f\bar{u} = -g\frac{\partial \zeta}{\partial y} - \frac{1}{\rho}\frac{\partial p_a}{\partial y} + \frac{G_S - G_B}{\rho D} + \frac{1}{\rho D}\frac{\partial}{\partial x}(DM_{xy}) + \frac{1}{\rho D}\frac{\partial}{\partial y}(DM_{yy}) \quad (1.20b)$$

with $$M_{xx} = \frac{1}{D}\int_{-h}^{\zeta}\left\{\tau_{xx} - \rho(u-\bar{u})^2\right\} dz$$

$$M_{xy} = \frac{1}{D}\int_{-h}^{\zeta}\left\{\tau_{xy} - \rho(u-\bar{u})(v-\bar{v})\right\} dz$$

$$M_{yy} = \frac{1}{D}\int_{-h}^{\zeta}\left\{\tau_{yy} - \rho(v-\bar{v})^2\right\} dz$$

being horizontal diffusion of momentum, where contributions from the vertical shear of the horizontal currents have been 'lumped in'. These are rather awkward terms but fortunately small and are accounted for if necessary by an effective horizontal eddy viscosity, A, so that

$$M_{xx} = -2\rho A\frac{\partial \bar{u}}{\partial x}$$

$$M_{xy} = M_{yx} = -\rho A\left\{\frac{\partial \bar{u}}{\partial y} + \frac{\partial \bar{v}}{\partial x}\right\}$$

$$M_{yy} = -2\rho A\frac{\partial \bar{v}}{\partial y}$$

Heaps (1978) then shows that

$$\frac{1}{\rho D}\frac{\partial}{\partial x}(DM_{xx}) + \frac{1}{\rho D}\frac{\partial}{\partial y}(DM_{yx}) \simeq A\nabla^2\bar{u}$$

and $$\frac{1}{\rho D}\frac{\partial}{\partial x}(DM_{xy}) + \frac{1}{\rho D}\frac{\partial}{\partial y}(DM_{yy}) \simeq A\nabla^2\bar{v}$$

when can be inserted in equation (1.20).

We have now reached the point where most of the equations required in shallow water have been derived.

2. Models

2.1 Types of Model

A model is an hypothesis, an approximation to the real world which attempts to capture the essence of a physical mechanism. Several types of model may be constructed, from the simplest mental image or back of the envelope calculation to a very sophisticated prediction system including as much of the physics as possible. The main types of model are analytical, physical and numerical.

2.2 Analytical models

These can be very powerful in terms of understanding the mechanism of the water movement but the equations usually have to be simplified and not all equations of interest have exact solutions. Simple topography i.e. boundary configuration and depths are usually required. Some examples of analytical models are now given.

(i)

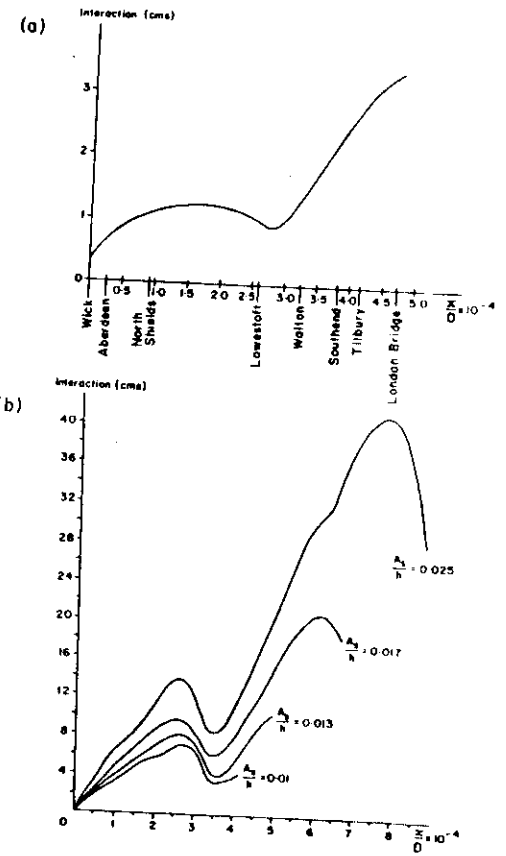

Fig. 2.1
Wace (1978)

Figure 2 shows how a simple 1-D channel model was used to explain the observed minimum in surge-tide interaction at Lowestoft in the North Sea. Progressive waves solutions $f(x-ct)$ and $g(x+ct)$ were introduced as the first order solution in the nonlinear surge/tide equations (c is wave phase speed $=\sqrt{gh}$).

(ii) Insight can be obtained into the nature of <u>wind-driven flow</u> by examining the linearised shallow water equations, i.e. ignoring the advective terms. Further simplifications must be made to obtain solutions, e.g.

if (a) coastal boundaries are sufficiently far away, $\zeta = 0$
(b) depth sufficiently deep that bottom friction negligible
(c) steady state has been achieved, no time derivatives

then
$$-fV = 0$$
$$fU = \frac{G_S}{\rho} = u_*^2 \qquad \text{where } u_* \text{ is here defined as the wind friction velocity}$$
$$\frac{\partial U}{\partial x} + \frac{\partial V}{\partial y} = 0 \qquad (2.1)$$

where $U = h\bar{u} = \int_{-h} u\,dz$, $V = h\bar{v} = \int_{-h} v\,dz$

are the x and y components of the total transport, we have a solution $U = \frac{G_S}{\rho f} = \text{constant}$, $V = 0$, the classical <u>Ekman transport</u> with transport being 90° to the right of the wind direction. The full vertical variation of current can be obtained if a constant vertical eddy viscosity is assumed. Then

$$-fv = N_z \frac{d^2u}{dz^2}$$
$$fu = N_z \frac{d^2v}{dz^2} \qquad (2.2)$$

Taking boundary conditions $N_z \frac{du}{dz} = 0$, $N_z \frac{dv}{dz} = 0$ at $z=0$ and $\frac{du}{dz} = \frac{dv}{dz} = 0$ at $Z \to -\infty$. We introduce the Ekman depth $= \sqrt{2N_z/f}$ and the solution is

$$\frac{u}{u_*} = \frac{u_*}{fd} e^{z/d} \left(\cos\frac{z}{d} - \sin\frac{z}{d}\right)$$
$$\frac{v}{u_*} = \frac{u_*}{fd} e^{z/d} \left(\cos\frac{z}{d} + \sin\frac{z}{d}\right) \qquad (2.3)$$

It is assumed for this example that these equations apply has a logarithmic current profile (this model will not be discussed here), because it is unrealistic to apply a constant eddy viscosity right up to the sea surface. This layer may be of the order of 1m thick. At the level here designated $z=0$, we have $u = v$ so the current is at 45° to the wind.

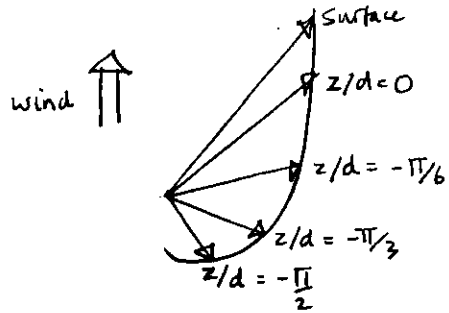

Fig. 2.2 Hodograph of horizontal velocity vectors at different depths relative to Ekman depth, d.

(iii) <u>Coastal setup</u> In the presence of a coastline at $x=0$ elevations can no longer be assumed to be zero. If the <u>wind is onshore</u>, assuming a <u>steady state</u> and <u>no along-shore gradients</u>, plus <u>zero velocity normal to the coast</u> we obtain

$$\frac{\partial \zeta}{\partial x} = \frac{F_S}{\rho g h} \quad , \quad \bar{u} = \bar{v} = 0, \qquad (2.4)$$

which implies a set-up at the coast (and for mass conservation, a set-down offshore).

If the <u>wind is alongshore</u> the balance is then between coriolis and the elevation gradient in the x-direction. Bottom friction must be retained to balance the surface stress in the y-direction. We assume a linear friction law $G_B = K\bar{v}$ where K = constant. Assume normal flow to coast is zero again, $\bar{u} = 0$.

$$\frac{K\bar{v}}{h} = \frac{G_S}{\rho h}$$
$$-f\bar{v} = -g\frac{\partial \zeta}{\partial x}$$
ie.
$$\frac{f}{K}\frac{G_S}{\rho} = g\frac{\partial \zeta}{\partial x} \quad \text{or} \quad \frac{\partial \zeta}{\partial x} = \frac{fh}{K}\frac{G_S}{\rho g h} \qquad (2.5)$$

Time varying solution

Circulation in the Coastal Ocean (Csanady, 1982)

Fig. 2.3

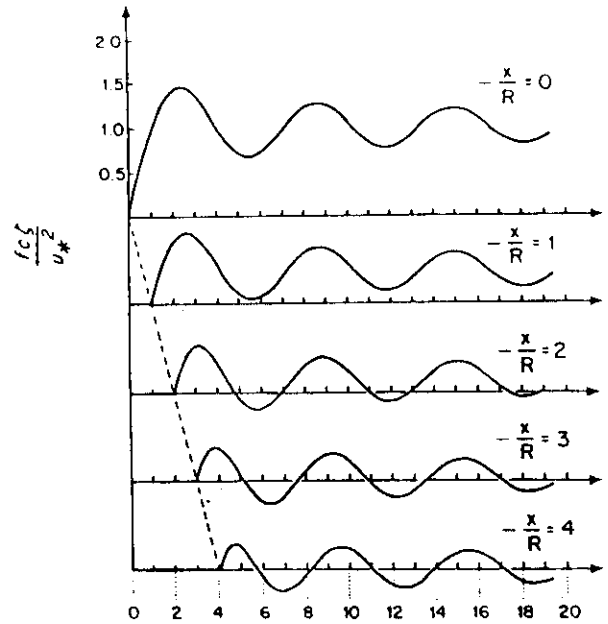

f1

Development of setup and oscillations due to cross-shore wind against an infinite coast. Beyond a few radii of deformation only oscillations arise. As in a closed basin, the level remains undisturbed until a pressure pulse arrives, travelling offshore at the speed $c = fR$. (Redrawn from Crépon, 1967).

The above figure is taken from Csanady (1982) and shows results obtained by Crépon (1967) for the time development of setup at different distances from the coast. An infinitely long straight coast in the y-direction has been assumed, no bottom friction and no alongshore gradient of elevation. The solution was obtained using Laplace transform methods. Some of the previous restrictions about proximity to the coast, zero transport and no time variation have been relaxed.

2.3 Physical Models

These have the advantage of direct reproduction of physical processes without parametisation of sub-grid scale physics in particular. However the benefits are counteracted by problems of scaling and the expense of producing such a model. Large scale models of specific estuaries and harbours are being increasingly replaced by numerical models. The model typically is designed for a particular application, however general-purpose facilities such as wave tanks may also be considered in this category. An example of such a model is given in Falconer and Mardapitta-Hadjipandeli (1987).

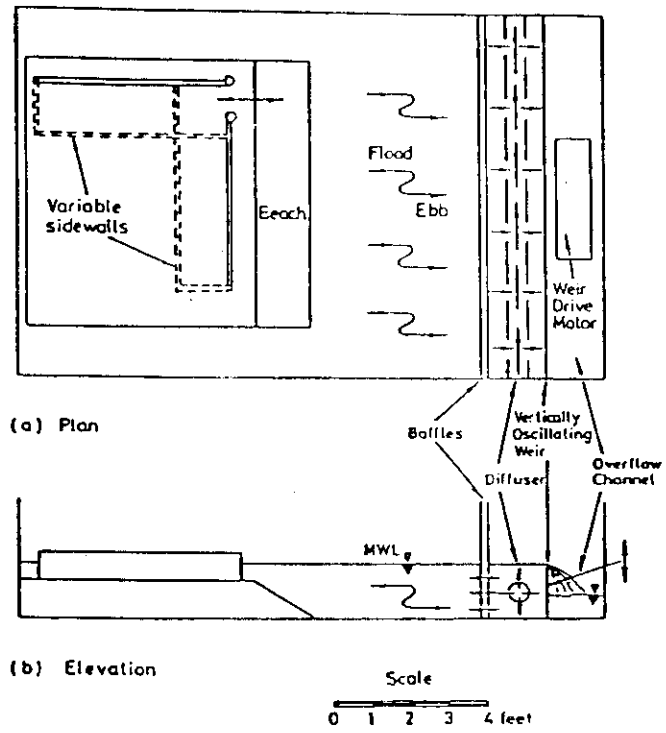

Details of Laboratory Tidal Tank and Harbour Configuration

Fig. 2.4

2.4 Numerical Models

These have the advantage of being able to tackle equations without analytical solutions. They can be simplified and idealised models to examine an aspect of the physics or highly complex to produce the best forecasting results. The problems can arise because of the approximations which have to be made to solve the equations numerically. Many techniques may be used which have individual merits and demerits. We will concentrate on this group of models. Note that physical and analytical models are very useful to test numerical models and vice versa.

2.5 Types of Partial Differential Equation (p.d.e.)

The generalised 2-dimensional (2D) linear pde is

$$au_{xx} + 2bu_{xy} + cu_{yy} + 2du_x + 2eu_y + fu = h(x,y), \quad (2.6)$$

with u any dependent variable.

If $b^2-ac < 0$ the equation is elliptic,
$b^2-ac = 0$ the equation is parabolic,
$b^2-ac > 0$ the equation is hyperbolic.

Some common elliptic equations are:-

Laplace's equation $$\frac{\partial^2 u}{\partial x^2} + \frac{\partial^2 u}{\partial y^2} + \frac{\partial^2 u}{\partial z^2} = 0 \quad (2.7)$$

Poisson's equation $$\frac{\partial^2 u}{\partial x^2} + \frac{\partial^2 u}{\partial y^2} + \frac{\partial^2 u}{\partial z^2} = -g(x,y,z) \quad (2.8)$$

These are generally steady-state bounary-value problems. Methods of solution include iterative or direct matrix inversion. Finite elemnt methods are particularly suited to this type of problem.

Parabolic equations:-

e.g Diffusion equation $$\frac{\partial u}{\partial t} = \alpha \frac{\partial^2 u}{\partial x^2} \qquad (\alpha = \text{diffusion coefficient})$$

This may be used in the vertical dimension in particular in transport models. Some finite difference solution methods include Crank-Nicholson and Lax-Wendroff.

Hyperbolic equation:-

e.g. Wave equation $$\frac{\partial^2 u}{\partial t^2} - c^2 \frac{\partial^2 u}{\partial x^2} = g(x) \quad (2.9)$$

which may be written as a system of first order equations

$$\left.\begin{aligned} \frac{\partial u}{\partial t} &= c\frac{\partial v}{\partial x} + tg \\ \frac{\partial v}{\partial t} &= c\frac{\partial u}{\partial x} \end{aligned}\right\} \quad (2.10)$$

if c is a constant phase speed. These are time-evolving problems.

Specific solution methods have been developed for each type of problem. We will mainly be looking at the solution of hyperbolic equations.

2.6 Finite element methods (FEM)

A variational approach is used to transform the equations. The solution is approximated by a weighted sum of selected basis functions, which is solved effectively by minimisation of energy. The domain is divided up by a grid with an arbitrary distribution of nodes at which the solution is obtained. The method is not described in further detail here, but examples are given in §4 of 3D models which use the FEM (termed the Galerkin method) in the vertical dimension.

Some advantages of the technique are variable element shape allowing good boundary fitting (triangles are often used). The variable resolution means that a fine grid can be applied where needed and a coarser grid elsewhere. However it is generally more time-consuming to set up and more expensive in computational effort than the finite difference method. The solution is built up out of simple basis functions which makes it smoother than the finite difference solution. For tidal modelling the time variation can be removed by transforming into the spectral domain using the tidal periodicities. This converts a hyperbolic problem to a set of elliptic equations (for which the finite element method is more naturally suited). For an example of the FEM and a discussion of its capabilities see e.g. LeProvost (1986). Some of the results of this are shown here.

The improvement of the solution, when using finer grids and higher degree basic elements,is clearly illustrated in Figure15.

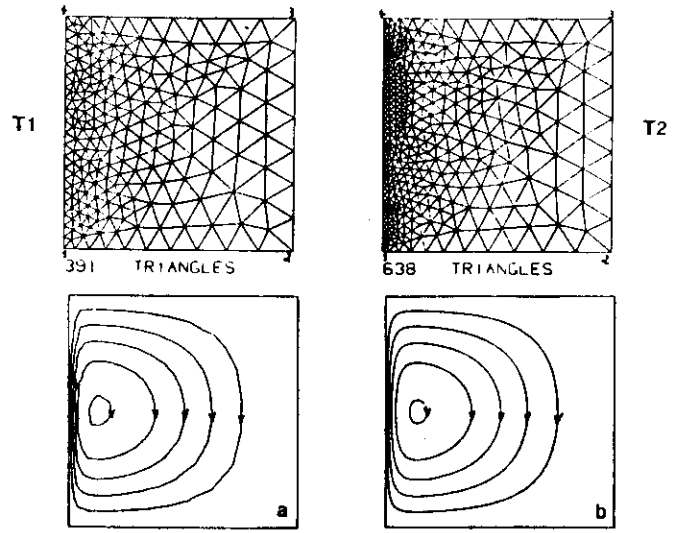

Figure15. Examples of steady state solution for the Stommel's linear case with dissipation by bottom friction (ϵ = 0.03) and slip boundary

2.7 Finite Difference (f.d.) Methods

In this case the solution domain is divided into a uniform grid of discrete points. In each grid-box the solution is assumed constant. The partial derivatives are replaced by differences between the solutions at nearby grid-points. The smaller the grid spacing, the closer the approximation should be to the real solution. Various options are available as to how to calculate the differences, whether centered or biased to one side or the other and selecting the right combination is essential to obtaining a correct solution. See Noye (1978) for a thorough review. As an example we will look at the 1-D diffusion equation for which the grid is shown in the figure 2.6.

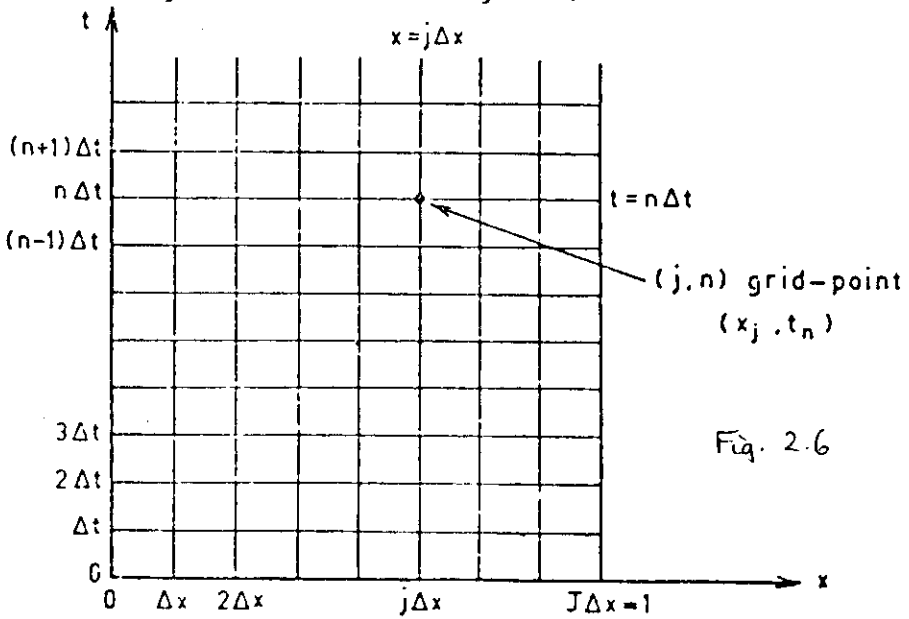

Fig. 2.6

$$\frac{\partial T}{\partial t} = \alpha \frac{\partial^2 T}{\partial x^2} \qquad (2.11)$$

$\frac{\partial T}{\partial t}$ may be rewritten $\frac{T_j^{n+1} - T_j^n}{\Delta t}$ at time $t = n\Delta t$, position $x = j\Delta x$

The approximation may be derived from a Taylor series expansion of the solution near the point x,t

$$T(x, t+\Delta t) = T(x,t) + \Delta t \left[\frac{\partial T}{\partial t}\right]_{x,t} + \frac{\Delta t^2}{2!}\left[\frac{\partial^2 T}{\partial t^2}\right]_{x,t} + O(\Delta t^3) \qquad (2.12)$$

This is called a forward-difference approximation and has truncation error $O(\Delta t)$ i.e. it is first-order accurate. We could have written $\frac{\partial T}{\partial t} = \frac{T_j^n - T_j^{n-1}}{\Delta t}$

which is a backward difference of the same order or

$$\frac{\partial T}{\partial t} = \frac{T_j^{n+1} - T_j^{n-1}}{2\Delta t} = \frac{1}{2\Delta t}\left\{ T_j^n + \Delta t\left[\frac{\partial T}{\partial t}\right]_j^n + \frac{\Delta t^2}{2!}\left[\frac{\partial^2 T}{\partial t^2}\right]^n + O(\Delta t^3) \right.$$
$$\left. - T_j^n + \Delta t\left[\frac{\partial T}{\partial t}\right]^n - \frac{\Delta t^2}{2!}\left[\frac{\partial^2 T}{\partial t^2}\right]^n + O(\Delta t^3) \right\} \qquad (2.1$$

This is called a 'central-difference' approximation because it is centered in time and is of the order (Δt^2) which is smaller than errors of $O(\Delta t)$.

The second order derivative can be approximated in the same way, by examining the Taylor series,

e.g. $$\left[\frac{\partial^2 T}{\partial x^2}\right]_j^n = \frac{T_j^{n+1} - 2T_j^n + T_j^{n-1}}{(\Delta x)^2} \qquad (2.14)$$

which is a central difference approximation with error $O(\Delta x^2)$.

When all the partial derivatives have been replaced in an equation by finite difference approximations the solution becomes a problem of solving a set of simultaneous equations (matrix algebra) $\underset{\sim}{X}^{t+\Delta t} = M . \underset{\sim}{X}^t$ (2.15)

A possible finite difference approximation for the diffusion equation would be

$$T_j^{n+1} = \alpha \frac{\Delta t}{(\Delta x)^2}\left(T_{j+1}^n + T_{j-1}^n\right) + \left(1 - 2\alpha \frac{\Delta t}{(\Delta x)^2}\right) T_j^n \qquad (2.16)$$

which is the classical forward in time, centred in space, FTCS method.

2.8 Consistency, Convergence and Stability

A useful finite difference scheme must satisfy the criteria of consistency, convergence and stability.

Consistency implies that in the limit as the grid spacing reduces to zero the finite difference equation must become closer and closer to the original p.d.e. i.e. the truncation error tends to zero as Δx, Δy, Δz, Δt tend to zero.

Convergence requires that the solution of the difference equation must converge to the solution of the p.d.e in the limit as the grid size is reduced to zero.

Stability is a very important requirement of the finite difference scheme, and is concerned with the propagation and accumulation of errors as the calculation proceeds. There will always be some numerical errors due to rounf-off in the computer because an infinite number of decimal places cannot be retained. In some f.d schemes which can be produced the errors can grow to the point where they completely mask the solution.

Lax's eqivalence theorem states that convergence and stability are equivalent for a consistent f.d. scheme, providing that the initial value problem is well-posed and that the problem is linear. Well-posed implies that the solution of the p.d.e must depend continuously on the initial conditions.

Stability Analysis

Various methods are available for testing stability of a f.d scheme, which examine the amplification effect of the finite

difference equations on introduced errors, some directly, as with the discrete perturbation method or the matrix method (which examines the eigenvalues of the matrix produced from the finite difference equations). The most commonly used method is Von Neumann's analysis which looks at the Fourier components of the error distribution. However it gives no information on the influence of boundary conditions which the matrix method can give.

Looking at the diffusion equation again

$$ {}^{*}T_j^n = T_j^n + \xi_j^n \qquad \text{where } {}^{*}T_j^n \text{ is the numerical approximation to the true solution } T_j^n \text{ with error } \xi_j^n $$

$$ {}^{*}T_j^{n+1} = s\left({}^{*}T_{j-1}^n + {}^{*}T_{j+1}^n\right) + (1-2s)\,{}^{*}T_j^n \text{, with } s = \frac{\alpha\Delta t}{(\Delta x)^2} $$

$$ \therefore \qquad \xi_j^{n+1} = s\left(\xi_{j-1}^n + \xi_{j+1}^n\right) + (1-2s)\,\xi_j^n \qquad (2.17) $$

write the error as a sum of Fourier components

$$ \xi_j^0 = \sum_{m=1}^{J} a_m \exp(i m \pi r_j \Delta x) \qquad i = \sqrt{-1} $$

(ξ_j^0 is the initial error). Studying one Fourier component is sufficient since the problem is linear. Therefore we introduce an error of the form

$$ \xi_j^n = A^n e^{i\theta_j} \qquad \text{where } \theta_j = j\pi\Delta x $$

Substitution into the f.d. equation gives

$$ A^{n+1} = A^n\left(s e^{-i\theta} + (1-2s) + s e^{i\theta}\right), \quad \theta = \pi\Delta x \qquad (2.18) $$

Define $A^{n+1} = G.A^n$ with G the amplification factor. The method is stable if $|G| \le 1$ for all θ.
In this example

$$ G = 1 - 2s + s\left(e^{i\theta} + e^{-i\theta}\right) = 1 - 4s\sin^2\theta/2 \qquad (2.19) $$

For stability $\quad -1 \le 1 - 4s\sin^2\theta/2 \le 1$

This is satisfied if $s \le \frac{1}{2}$, i.e. $\Delta t \le \Delta x^2 / 2\alpha$.

2.9 Explicit vs implicit methods

The example FTCS method shown contains only one variable at the higher time level so the new value can be calculated from previously calculated values. This is therefore an explicit scheme. However more complex schemes can be devised which contain more than one variable at the higher time level. These cannot be solved point by point but require other techniques to invert the matrix. The advantage is that implicit schemes are more stable and can use longer time-steps. For example the classical implicit method uses backward differences in time.

$$ \frac{T_j^{n+1} - T_j^n}{\Delta t} = \alpha\left\{\frac{T_{j+1}^{n+1} - 2T_j^{n+1} + T_{j-1}^{n+1}}{(\Delta x)^2}\right\} \qquad (2.20) $$

Stability analysis shows this method to be unconditionally stable. The matrix is tri-diagonal and can be solved using the Thomas algoritm [Thomas (1949)] which is more efficient than inverting the whole matrix e.g. by Gaussian elimination. Other methods include the DuFort-Frankel method

$$ \frac{T_j^{n+1} - T_j^{n-1}}{2\Delta t} = \alpha\left\{\frac{T_{j+1}^n - \left(T_j^{n+1} + T_j^{n-1}\right) + T_{j-1}^n}{(\Delta x)^2}\right\} \qquad (2.21) $$

This is central in time but need 2 previous time levels; another method e.g. FTCS must be used for the first time-step. The equation can be rearranged to solve explicitly and is unconditionally stable, however $\Delta t < \Delta x$ is required for consistency. The Crank-Nicholson for 1-D diffusion can be useful to get high resolution in the vertical dimension. This uses central differences centred on a point midway between two grid-points.

$$ \frac{T_j^{n+1} - T_j^n}{\Delta t} = \frac{1}{2}\alpha\left\{\frac{T_{j+1}^{n+1} - 2T_j^{n+1} + T_{j-1}^{n+1}}{(\Delta x)^2} + \frac{T_{j+1}^n - 2T_j^n + T_{j-1}^n}{(\Delta x)^2}\right\} \qquad (2.22) $$

In multiple dimensions other methods are needed. Some implicit methods use iteration to obtain the solution e.g. S.O.R. (successive over-relaxation). The alternating-direction-implicit technique also uses the Thomas algorithm to get a fast solution while retaining the advantages of longer time steps.

This is only a sample of the f.d. methods which may be constructed to give an idea of the possibilities and the drawbacks, particularly of using a first-guess approach.

3. Finite difference modelling.

3.1 An explicit 2D tide/surge model

We will concentrate here on the explicit f.d. method applied to the depth-averaged equations for tides and surges on the continental shelf. We will discuss further details of finite difference techniques relevant to implementation of the U.K. surge forecasting model. Development of this model has involved various people at P.O.L. (previously I.O.S. Bidston) over many years, in particular Norman Heaps and Roger Flather. The operational model grid (now being superceded by a finer mesh)

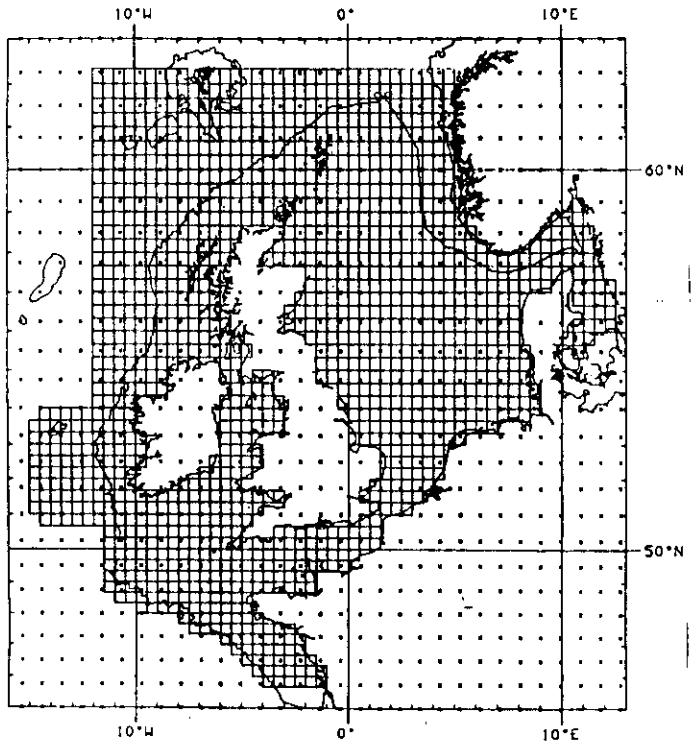

Fig 3.1 Finite difference grid of the operational storm surge forecast model with pressure points (x) of the Met. Office 15-level weather prediction model.

is shown in Figure 3.1

The equations to be solved are the fully nonlinear depth-averaged equations of motion and continuity. In Cartesian coordinates they are

$$\frac{\partial (Du)}{\partial x} + \frac{\partial (Dv)}{\partial y} + \frac{\partial \zeta}{\partial t} = 0 \qquad (3.1)$$

$$\frac{du}{dt} - fv + g\frac{\partial \zeta}{\partial x} = -\frac{1}{\rho}\frac{\partial p_a}{\partial x} + \frac{\tau_S - \tau_B}{\rho D} + A_x \qquad (3.2)$$

$$\frac{dv}{dt} + fu + g\frac{\partial \zeta}{\partial y} = -\frac{1}{\rho}\frac{\partial p_a}{\partial y} + \frac{G_S - G_B}{\rho D} + A_y \qquad (3.3)$$

(The overbar denoting depth-averaged quantities has been omitted). A_x, A_y are the horizontal shear stress terms.

3.2 Coordinate system

For an area as large as the UK continental shelf it is necessary to take account of the Earth's curvature. This means that the Cartesian coordinate system is no longer adequate. A more appropriate orthogonal coordinate system is spherical polar coordinates. In this case the equations (3.1) to (3.3) become

$$\frac{1}{R\cos\phi}\left\{\frac{\partial}{\partial \chi}(Du) + \frac{\partial}{\partial \phi}(Dv\cos\phi)\right\} + \frac{\partial \zeta}{\partial t} = 0 \qquad (3.4)$$

$$\frac{\partial u}{\partial t} + \frac{u}{R\cos\phi}\frac{\partial u}{\partial \chi} + \frac{v}{R}\frac{\partial u}{\partial \phi} - v\left\{f + u\frac{\tan\phi}{R}\right\} = -\frac{g}{R\cos\phi}\frac{\partial \zeta}{\partial \chi} - \frac{1}{\rho R\cos\phi}\frac{\partial p_a}{\partial \chi} + \frac{F_S - F_B}{\rho D} + A_x \qquad (3.5)$$

$$\frac{\partial v}{\partial t} + \frac{u}{R\cos\phi}\frac{\partial v}{\partial \chi} + \frac{v}{R}\frac{\partial v}{\partial \phi} + u\left\{f + u\frac{\tan\phi}{R}\right\} = -\frac{g}{R}\frac{\partial \zeta}{\partial \phi} - \frac{1}{\rho R}\frac{\partial p_a}{\partial \phi} + \frac{G_S - G_B}{\rho D} + A_y \qquad (3.6)$$

where χ is longitude and ϕ is latitude.

3.3 Nonlinear effects

It is usual to use a nonlinear friction term in the surge model because the linear form is unrealistic in shallow water with large tidal currents where friction is very important. The friction term is discussed in § 3.8.

Other nonlinearities are introduced by using the total water depth $D = h + \zeta$ in the continuity equation and the friction term and by retaining the advective terms. Introducing nonlinear terms in the finite difference equation means the stability analysis no longer holds although some guidance can be obtained. As long as the nonlinear terms are not too large the scheme may remain stable and certain techniques have been found useful for handling the nonlinear terms. The equations may be linearised which allows for direct comparison with analytic methods as well as simplifying the f.d. solution. Which terms can be ignored can be tested by dimensional analysis. The advective terms may often be ignored on the shelf scale but in fine-resolution local models they may be important. Linearising the friction terms requires scaling the constant by a 'typical' velocity (usually the M_2 tidal amplitude) to ensure sufficient damping.

3.4. Initial and boundary conditions

Since we are solving a time-stepping problem an initial state for the dependent variables must be specified. The initial conditions should ideally be as accurate as possible however initial errors are transient because friction tends to damp them out. If the tidal solution only is required the model can be run until a steady periodic state is reached. However if the transient effects are important eg. for Surge modelling the initial conditions are more critical. The options are

(i) cold start ($u = v = \zeta = 0$)
(ii) restart (use final value from previous run)
(iii) initialising with assimilated observed data if available

2 main types of boundary condition are recognised:

(i) Dirichlet condition ie. boundary value specified
(ii) Neumann condition ie. the normal derivative at the boundary is specified.

In particular, it is usual to set the velocity at a land boundary, normal to the coast, to be zero.

i.e. $$\underset{\sim}{q} \cdot \underset{\sim}{n} = 0 \qquad (3.7)$$

where $\underset{\sim}{n}$ is the vector normal to the coast. The coastline is usually specified as a 'staircase', producing a model coastline not exactly coincident with the real coastline eg.

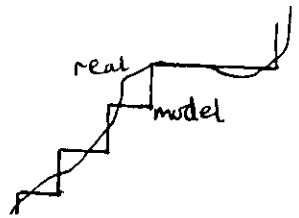

Fig. 3.2

but more sophisticated methods can be attempted including a moving coastline due to inundation and drying, which is most relevant to fine-resolution coastal models, eg. Flather and Hubbert (1990).

The open boundary condition is quite a difficult problem. The ideal boundary is perfectly transparent to all wavelengths, acting as if the model were connected to the external water mass, but this cannot be achieved and boundary conditions tend to be tailored to specific problems. Various boundary conditions are reviewed by Reed & Cooper (1986) including several types of radiation condition derived from the Sommerfeld radiation condition [Sommerfeld, 1949) stating that

$$Q_t = c_Q Q_n \qquad (3.8)$$

where Q is any dependent variable and c_Q is the phase speed of waves reaching the boundary. Accuracy of the boundary condition must also be traded against computational effort. Determination of the optimum phase speed can be difficult. The surge model uses 2 types of boundary condition:-

(i) elevation (or current) specified
(ii) a radiation condition with $c_Q = \sqrt{gh}$ the gravity wave speed which deals with most of the outgoing energy satisfactorily. The boundary is taken at the shelf edge so that in part, it is well away from the regions of interest

If $\hat{\zeta}, \hat{q}_n$ are the elevation and current prescribed values at the boundary Γ_b we have

(i) $$\zeta = \hat{\zeta} \quad , \Gamma_b \quad \text{or} \quad q_n = \hat{q}_n \quad , \Gamma_b \qquad (3.9)$$

(ii) $$q_n = \hat{q}_n + \sqrt{\frac{g}{D}}(\zeta - \hat{\zeta}) \quad , \Gamma_b \qquad (3.10)$$

Another way of dealing with open boundary is to nest fine-grid models within larger-area coarser-grid models and use the outer model to provide boundary conditions for the inner model. Usually the information transfer is one-way but 'dynamic nesting' can be attempted.

Where to put the boundary depends on:

(i) the physics ie. if there is a natural boundary to a system it should be the first choice
(ii) computer capacity ie. high resolution models are of necessity limited-area because they are more time-consuming

3.5 Grid selection

The dependent variables need not all be specified at the same grid-point and in fact staggering the grid can lead to improvement of the accuracy of the finite difference formulation for a given resolution or grid-spacing. Three standard grid layouts are identified (Mesinger & Arakawa, 1976)

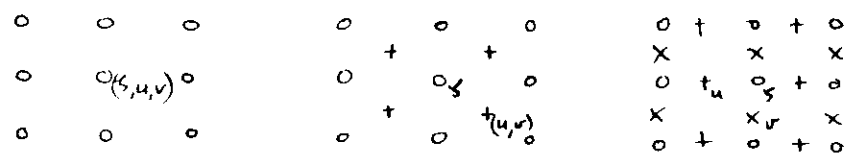

A-grid B-grid C-grid

o = ζ-point + = u or (u,v)-point x = v-point

Figure 3.3

For the linearised non-rotating equations the C-grid is preferable :—

$$\left.\begin{aligned} \frac{\partial \zeta}{\partial t} + h\frac{\partial u}{\partial x} + h\frac{\partial v}{\partial y} &= 0 \\ \frac{\partial u}{\partial t} + g\frac{\partial \zeta}{\partial x} + Ku &= 0 \\ \frac{\partial v}{\partial t} + g\frac{\partial \zeta}{\partial y} + Kv &= 0 \end{aligned}\right\} \qquad (3.11)$$

where K is the linear friction coefficient. Elevation spatial gradients are required at the u- and v-points but not the actual elevation values. Similarly only the x-derivative of u and the y-derivative of v are required at the ζ-points.

Once other terms like Coriolis, nonlinear friction and the advective terms are introduced the C-grid requires some interpolation of values which degrades the solution in particular smoothing out large values and strong gradients. To implement Coriolis on the C-grid means averaging the 4 nearest v-points onto a u-point and vice versa.

It has been found that where advection is important the B-grid is preferable eg. James (1959).

The grid size must be small enough to resolve the physics of interest. Usually a minimum of 10 grid points per wavelength is advised. Consideration must also be made of resolution of relevant topography.

3.6 Tides and Surges

Tides are a periodic motion driven by the gravitational attraction of the sun and moon and locked into the periodicities of their orbits. In shallow seas the tides are mainly driven by pressure gradients set up by the oceanic tides, the direct tide-generating-force being negligible. Therefore the tides need to be specified accurately on the boundary of a tidal model for a shallow sea area. Tidal currents should also be specified if possible, using the radiation boundary condition.

Surges are caused by non-astronomical effects, mainly meteorological forcing. There is also a component defined as surge (= non-tidal residual) which is due to nonlinear interactions between surge and tide. The meteorological forcing is paramount for surge prediction.

3.7 Wind forcing and atmospheric pressure effects

A change in atmospheric pressure affects sea level. This is called the inverse barometer effect. The steady state solution gives

$$\left.\begin{aligned} -g\frac{\partial \zeta}{\partial x} - \frac{1}{\rho}\frac{\partial p_a}{\partial x} &= 0 \\ -g\frac{\partial \zeta}{\partial y} - \frac{1}{\rho}\frac{\partial p_a}{\partial y} &= 0 \end{aligned}\right\} \qquad (3.12)$$

ie. $\rho g\zeta + p_a = \text{constant}$

1 mb. change in atmospheric press. $\simeq$ 1 cm sea level.

However the wind-stress causes most of the surge response. Wind stress is usually parametrised in a similar way to bottom friction ie.

$$\left.\begin{aligned} F_s &= \rho_a C_D W_x\sqrt{W_x^2+W_y^2} \\ G_s &= \rho_a C_D W_y\sqrt{W_x^2+W_y^2} \end{aligned}\right\} \equiv \rho_a U_*^2 \qquad (3.13)$$

with ρ_a the density of air and C_D a drag coefficient. C_D is not a constant but increases with wind-speed. Various models are used for calculating wind stress. For the surge model a formula Smith and Banke (1975) has been found appropriate i.e. $C_D = (0.63 + 0.066|W|).10^{-3}$

Wind has most effect in shallower water as may be seen from the equations

$$\frac{\partial u}{\partial t} = \frac{F_S}{\rho D} + \ldots$$

the inverse depth effect means wind-driven depth-averaged currents are very small off the continental shelf. It is sufficient to prescribe the hydrostatic elevation (due to atmospheric pressure) at the boundary and the wind-driven flow is internal to the model. This makes the continental shelf edge a 'natural' boundary for the surge model.

3.8 Friction

A common parametrisation of the bottom friction term is the 'quadratic law' relating the stress to the depth mean velocity squared

$$F_B = k\rho u\sqrt{u^2+v^2} \quad , \quad G_B = k\rho v\sqrt{u^2+v^2} \qquad k = \text{'constant'} \approx 0.0025$$

This formulation is consistent with the eddy viscosity approach for the internal stresses, combined with the ubiquitous logarithmic velocity profile near the bed and using Prandtl's mixing-length hypothesis to parametrise the viscosity near the bottom. However it strictly only applies to near-bed currents and has been extended to use depth-mean currents of necessity, (see §4).

If $u = \frac{u_*}{\kappa z_0}\ln\left(\frac{z+h}{z_0}\right)$ is the standard logarithmic (3.14)

profile near the sea-bed, z_0 is a roughness length characterising the sea bed, u_* is the bed friction velocity and κ is von Karman's constant $= 0.4$, taking $N_z = l^2|\partial u/\partial z|$ with $l = \kappa(z+h)$ a 'mixing length', we have

$$\tau_{zx}(-h+z_0) = \rho N_z \frac{\partial u}{\partial z} = \rho l^2 \frac{\partial u}{\partial z}\left|\frac{\partial u}{\partial z}\right| = \rho u_*^2 \qquad (3.15)$$

3.9 Finite difference solution

Some features of the finite difference scheme are as follows

(i) An explicit time-stepping procedure is used ie. only known values are used in each calculation

(ii) Forward time-stepping, centred spatial derivatives.

(iii) The highest time level velocities available are used in the Coriolis term (which involves 4-point averaging). The order of calculations is reversed each time-step. When new u values are calculated first, they are used in the following v-equation and vice versa. The reversal of order means the scheme is called 'alternating-direction explicit'.

(iv) The 'angled-derivative' method (Roberts and Weiss, 1966) is used for the advective terms. This allows them to be partially evaluated at the higher time level by using the order of passing through the grid, using the latest computed values.

(v) The friction term is partially time-centred by making the central velocity at the higher time level. The equation can then be reorganised and still solved explicitly.

eg. looking a simplified equation

$$\frac{\partial u}{\partial t} = -\frac{k u\sqrt{u^2+v^2}}{\rho D} \qquad (3.16)$$

we write

$$\frac{u_i^{n+1}-u_i^n}{\Delta t} = -\frac{k u_i^{n+1}\sqrt{u_i^{n2}+v_i^{n2}}}{\rho D_i^n} \qquad (3.17)$$

This can be rewritten

$$u_i^{n+1}\left(\frac{1}{\Delta t}+\frac{k\sqrt{u_i^{n2}+v_i^{n2}}}{\rho D_i^n}\right) = \frac{u_i^n}{\Delta t} \qquad (3.18)$$

The grid numbering system is shown in Figure 3.4 counting from the top left corner in a single increment. This allows reference to the full equations for computation, shown in Figure 3.5.

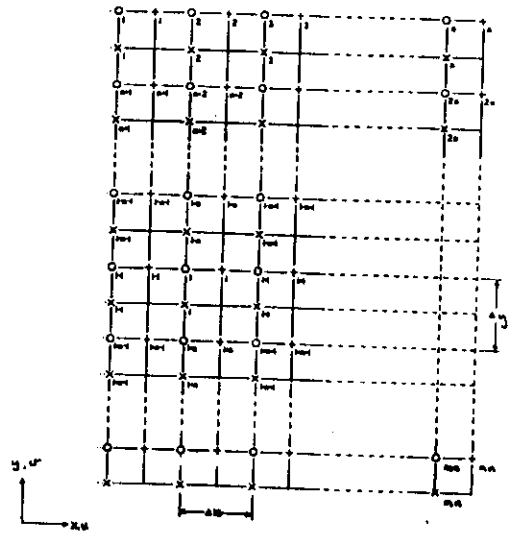

Figure 3.4

Continuity

$$\frac{\xi_i^{(n+1)} - \xi_i^{(n)}}{\tau}$$

$$+ \frac{1}{R \cos \Phi_m} \left\{ \frac{(d_i^{(n)} u_i^{(n)} - d_{i-1}^{(n)} u_{i-1}^{(n)})}{\Delta \chi} + \frac{(e_{i-n}^{(n)} \cos \Phi_{m-1} v_{i-n}^{(n)} - e_i^{(n)} \cos \Phi_{m+1} v_i^{(n)})}{\Delta \Phi} \right\} = 0 .$$

where τ is the time step,
$d_i = 0.5 (H_i + H_{i-1})$,
$e_i = 0.5 (H_i + H_{i-n})$.

Discrete values of the variables at appropriate grid points are identified by subscripts as follows

$\xi = \xi_i$, $h = h_i$, $H = H_i = h_i + \xi_i$ at ξ-point i,
$u = u_i$ at u-point i,
$v = v_i$ at v-point i.

Even timesteps : i decreasing

V-equation

$$\frac{v_i^{(n+1)} - v_i^{(n)}}{\tau}$$

$$= - 2 \omega \sin \Phi_{m+1} \bar{u}_i^{(n)} - \frac{\bar{v}_i^{(n)}}{2 \Delta \Phi R} [v_i^{(n+1)} + v_{i-n}^{(n)} - v_i^{(n)} - v_{i+n}^{(n+1)}]$$

$$- \frac{\bar{u}_i^{2(n)}}{R} \tan \Phi_{m+1} - \frac{1}{2 R \cos \Phi_{m+1}} \left\{ 0.5 [u_{i-1}^{(n)} + u_{i+n-1}^{(n)}] \frac{[v_i^{(n)} - v_{i-1}^{(n)}]}{\Delta \chi} \right.$$

$$\left. + 0.5 [u_i^{(n)} + u_{i+n}^{(n)}] \frac{[v_{i+1}^{(n)} - v_i^{(n+1)}]}{\Delta \chi} \right\}$$

$$- k v_i^{(n+1)} \frac{(\bar{u}_i^{2(n)} + v_i^{2(n)})^{1/2}}{e_i^{(n)}} - \frac{g}{R} \left\{ \frac{\xi_i^{(n+1)} - \xi_{i+n}^{(n+1)}}{\Delta \Phi} \right\} + \frac{1}{\rho} \left\{ - Q_i^{(n)} + \frac{G_i^{(n)}}{e_i^{(n)}} \right\}$$

U-equation

$$\frac{u_i^{(n+1)} - u_i^{(n)}}{\tau}$$

$$= 2 \omega \sin \Phi_m \bar{v}_i^{(n+1)} - \frac{\bar{u}_i^{(n)}}{2 \Delta \chi R \cos \Phi_m} [u_{i+1}^{(n+1)} + u_i^{(n)} - u_i^{(n+1)} - u_{i-1}^{(n)}]$$

$$+ \frac{u_i^{(n)} \bar{v}_i^{(n)}}{R} \tan \Phi_m - \frac{1}{2 R} \left\{ 0.5 [v_{i-n}^{(n)} + v_{i-n+1}^{(n)}] \frac{[u_{i-n}^{(n)} - u_i^{(n)}]}{\Delta \Phi} + 0.5 [v_i^{(n)} + v_{i+1}^{(n)}] \frac{[u_i^{(n)} - u_{i+n}^{(n)}]}{\Delta \Phi} \right\}$$

$$- \frac{k u_i^{(n+1)} (u_i^{2(n)} + \bar{v}_i^{2(n)})^{1/2}}{d_i^{(n)}} - \frac{g}{R \cos \Phi_m} \frac{[\xi_{i+1}^{(n+1)} - \xi_i^{(n+1)}]}{\Delta \chi} + \frac{1}{\rho} \left\{ - P_i^{(n)} + \frac{F_i^{(n)}}{d_i^{(n)}} \right\} .$$

Odd timesteps : i increasing

U-equation

$$\frac{u_i^{(n+1)} - u_i^{(n)}}{\tau}$$

$$= 2 \omega \sin \Phi_m \bar{v}_i^{(n)} - \frac{\bar{u}_i^{(n)}}{2 \Delta \chi R \cos \Phi_m} [u_{i+1}^{(n)} + u_i^{(n+1)} - u_i^{(n)} - u_{i-1}^{(n+1)}]$$

$$+ \frac{u_i^{(n)} \bar{v}_i^{(n)}}{R} \tan \Phi_m - \frac{1}{2 R} \left\{ 0.5 [v_{i-n}^{(n)} + v_{i-n+1}^{(n)}] \frac{[u_{i-n}^{(n+1)} - u_i^{(n+1)}]}{\Delta \Phi} + 0.5 [v_i^{(n)} + v_{i+1}^{(n)}] \frac{[u_i^{(n)} - u_{i+n}^{(n)}]}{\Delta \Phi} \right\}$$

$$- \frac{k u_i^{(n+1)} (u_i^{2(n)} + \bar{v}_i^{2(n)})^{1/2}}{d_i^{(n)}} - \frac{g}{R \cos \Phi_m} \frac{[\xi_{i+1}^{(n+1)} - \xi_i^{(n+1)}]}{\Delta \chi} + \frac{1}{\rho} \left\{ - P_i^{(n)} + \frac{F_i^{(n)}}{d_i^{(n)}} \right\} .$$

V-equation

$$\frac{v_i^{(n+1)} - v_i^{(n)}}{\tau}$$

$$= - 2 \omega \sin \Phi_{m+1} \bar{u}_i^{(n+1)} - \frac{\bar{v}_i^{(n)}}{2 \Delta \Phi R} [v_i^{(n)} + v_{i-n}^{(n+1)} - v_i^{(n+1)} - v_{i+n}^{(n)}]$$

$$- \frac{\bar{u}_i^{2(n)}}{R} \tan \Phi_{m+1} - \frac{1}{2 R \cos \Phi_{m+1}} \left\{ 0.5 [u_{i-1}^{(n)} + u_{i+n-1}^{(n)}] \frac{[v_i^{(n+1)} - v_{i-1}^{(n+1)}]}{\Delta \chi} + 0.5 [u_i^{(n)} + u_{i+n}^{(n)}] \frac{[v_{i+1}^{(n)} - v_i^{(n)}]}{\Delta \chi} \right\}$$

$$- \frac{k v_i^{(n+1)} (\bar{u}_i^{2(n)} + v_i^{2(n)})^{1/2}}{e_i^{(n)}} - \frac{g}{R} \left\{ \frac{\xi_i^{(n+1)} - \xi_{i+n}^{(n+1)}}{\Delta \Phi} \right\} + \frac{1}{\rho} \left\{ - Q_i^{(n)} + \frac{G_i^{(n)}}{e_i^{(n)}} \right\} .$$

where $\bar{u}_i = 0.25 (u_i + u_{i-1} + u_{i+n-1} + u_{i+n})$,
$\bar{v}_i = 0.25 (v_i + v_{i+1} + v_{i-n+1} + v_{i-n})$,
$\bar{u}_i = 0.25 (u_{i+1} + 2 u_i + u_{i-1})$,
$\bar{v}_i = 0.25 (v_{i-n} + 2 v_i + v_{i+n})$,
$P_i = \frac{1}{R \cos \Phi} \frac{\partial p_a}{\partial \chi}$ at u-point i,
$Q_i = \frac{1}{R} \frac{\partial p_a}{\partial \Phi}$ at v-point i,
$F_i = F^{(n)}$ at u-point i, $= \tau_\chi(s)$
$G_i = G^{(n)}$ at v-point i. $= \tau_\varphi(s)$ } wind stress
$k = c_b$ – bottom friction parameter

Figure 3.5

The procedure to be followed in setting up a model run is shown in Fig. 3.6

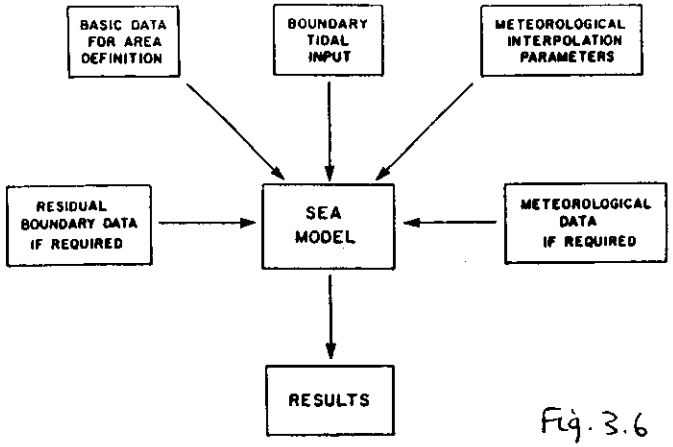

Fig. 3.6

The time-step has to be selected for stability since this is an explicit method. It turns out that

$$\Delta t < \frac{1}{\sqrt{gh}} \frac{\Delta x \Delta y}{\sqrt{(\Delta x)^2+(\Delta y)^2}} \left\{1 - \tfrac{1}{2}\Delta t \left(\frac{k}{h}+f\right)\right\}^{\frac{1}{2}}$$

and $$\Delta t < \frac{2}{K/h+f}$$

are required. If $\Delta x = \Delta y$, $K = f = 0$ this becomes

$$\Delta t < \frac{\Delta x}{\sqrt{2gh}}$$

which is known as the Courant-Friedrichs-Lewy (CFL) criterion, a useful guideline for choosing the timestep for an explicit model.

The model is actually run twice to produce a surge forecast

(i) tide only ie. $F_s, G_s, \frac{\partial p_a}{\partial x}, \frac{\partial p_a}{\partial y} = 0$

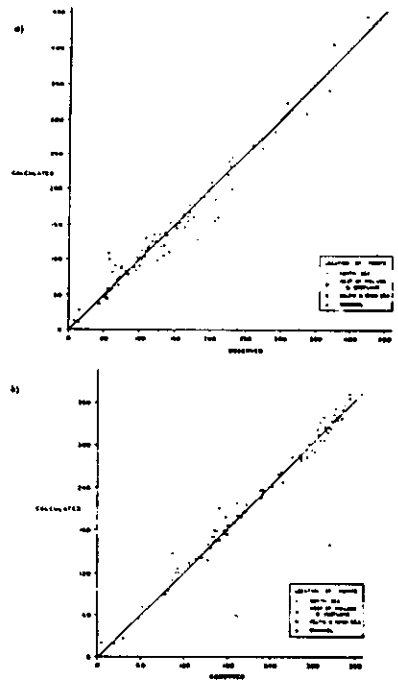

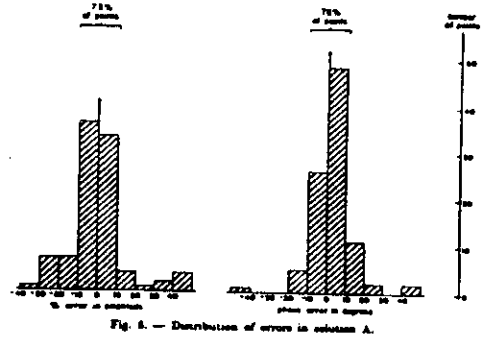

Fig. 6. — Distribution of errors in solution A.

Comparison of computed and observed harmonic constants (Flather 1976)

Figure 3.7

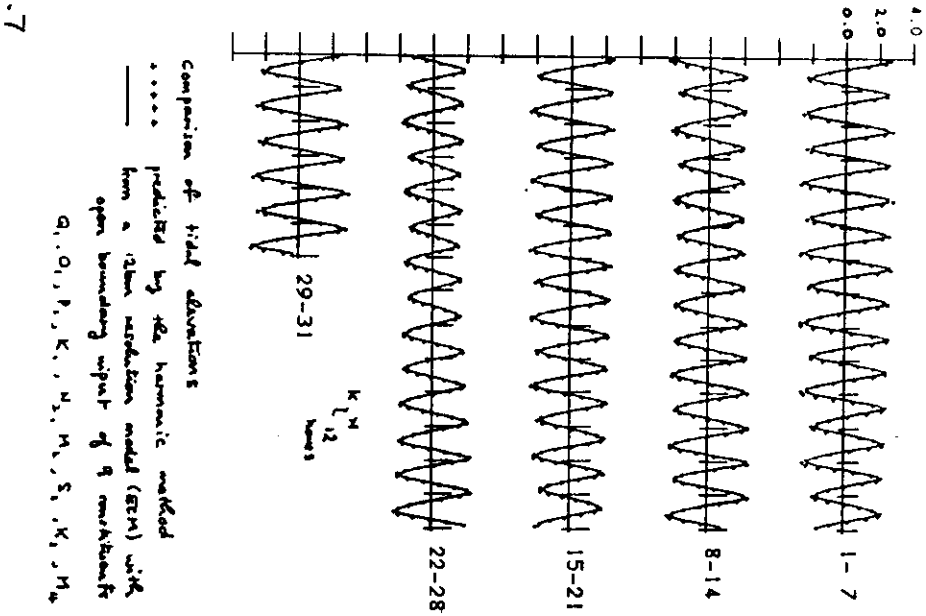

Southend July 1988

(ii) tide plus surge ie to allow surge-tide interaction
(iii) the final surge residuals are obtained from (ii) - (i)
Some examples of tidal calculations are shown in Figure 3.7 and some surge residuals in Figure 3.8, compared to observations.

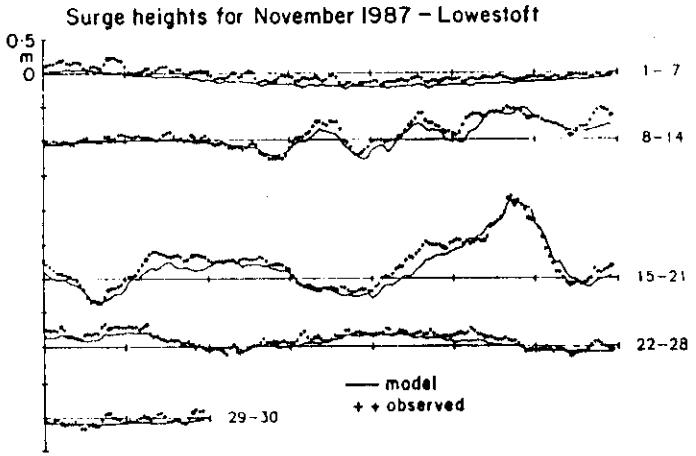

Figure 3.8